17th World Conference on Earthquake Engineering, 17WCEE
Sendai, Japan - September 13th to 18th 2020

CNN-BASED BUILDING DAMAGE DETECTION MODEL FOR THE PROMPT DISASTER RESPONSE UTILIZING REMOTE SENSING IMAGES

S. Naito[(1)], H. Nakamura[(2)], H. Fujiwara[(3)], H. Tomozawa[(4)], Y. Mori[(4)] , N. Monma[(5)]

[(1)] *Researcher, National Research Institute for Earth Science and Disaster Resilience, naito@bosai.go.jp*
[(2)] *Senior Researcher, National Research Institute for Earth Science and Disaster Resilience, manta@bosai.go.jp*
[(3)] *Manager, National Research Institute for Earth Science and Disaster Resilience, fujiwara@bosai.go.jp*
[(4)] *Mizuho Information & Research Institute, Inc.*
[(5)] *PASCO Corporation*
…

Abstract

Following an earthquake, an estimation of the damage suffered by buildings is useful for disaster response. To this end, the Japan real-time information system for earthquakes (J-RISQ) has been developed. However, the resolution of the data or uncertainties in the estimation models mean that the estimation results do not always correspond to the actual damage. Thus, information must be aggregated using remote sensing and the estimation results updated. This is extremely labor-intensive if done by human judgment. Therefore, we developed an automatic building damage classification model based on a convolutional neural network (CNN) that uses remote sensing images.

The initial training data came from damaged buildings. Using aerial photos taken soon after the 2016 Kumamoto earthquake, we classified the damage to each building into four levels. Subsequently, approximately 320,000 GIS data labeled with these four damage levels were used as training data. By comparing the classification results with field inspection results, the visual interpretation of aerial photographs was found to be superior at detecting collapsed buildings.

Using these training data, 80×80-pixel image patches were cropped from the aerial photos. We developed a CNN-based damage detection model, and trained this model with the cropped image patches. By applying the model to 20 aerial photographs of the aftermath of the Kumamoto earthquake, all buildings were automatically classified into the four damage levels. Furthermore, we compared this CNN-based classification result with a visual interpretation of the same area, and confirmed that the accuracy of CNN discrimination can be used to prioritize manpower and other resources.

In the early stages of disaster response, accessible aerial images are not readily available. Thus, we combined this model with a Bayesian updating method, whereby the estimation result given by J-RISQ is updated using the CNN-based damage detection model. In the case of the Kumamoto earthquake, the J-RISQ results overestimated the damage in Kumamoto city compared with a governmental field survey. However, by using the proposed updating method with aerial photos, we produced estimation results for Kumamoto city that were closer to the governmental survey result. Therefore, we believe this method is suitable for supporting the disaster response efforts of government departments and insurance companies.

Keywords: Damage detection, Remote Sensing, Deep learning, Convolutional Neural Network

1. Introduction

To support the disaster response efforts performed by government agencies and companies, it is vital to estimate the damage suffered by buildings immediately after large earthquakes. For this purpose, the Japan real-time information system for earthquakes (J-RISQ) was developed [1]. J-RISQ estimates the damage to buildings approximately 10 minutes after the earthquake, using seismic records from more than 5,000 strong motion sensors. Additionally, J-RISQ uses geomorphological data of site-amplifications and building-attribution data with a resolution of 250 m covering the whole of Japan [2]. However, the estimation results produced by J-RISQ do not always correspond to the actual damage. This is primarily because of the density of the observation stations, the resolution of site-amplification data, and the uncertainties of damage estimation models based on fragility curves. Thus, it is necessary to update the estimation results using observed damage information [3].

Remotely sensed images taken by satellites, airplanes, and UAVs are available for highly damaged areas. However, when the affected area covers a large extent, obtaining an overall picture of the disaster is very labor-intensive. Automatic damage detection models using machine learning are highly effective for prompt disaster response. Recently, many machine learning methods using remote sensing images have been applied to the detection of damage in buildings [4] [5]. Among them, a convolutional neural network (CNN) [6] achieved especially high performance using a large number of training data [7][8][9]. Therefore, in a previous study, we developed a CNN-based building damage detection model that uses post-earthquake aerial photography [10]. In this study, we used this model to update the J-RISQ estimation results for the purpose of supporting prompt disaster response (Fig. 1).

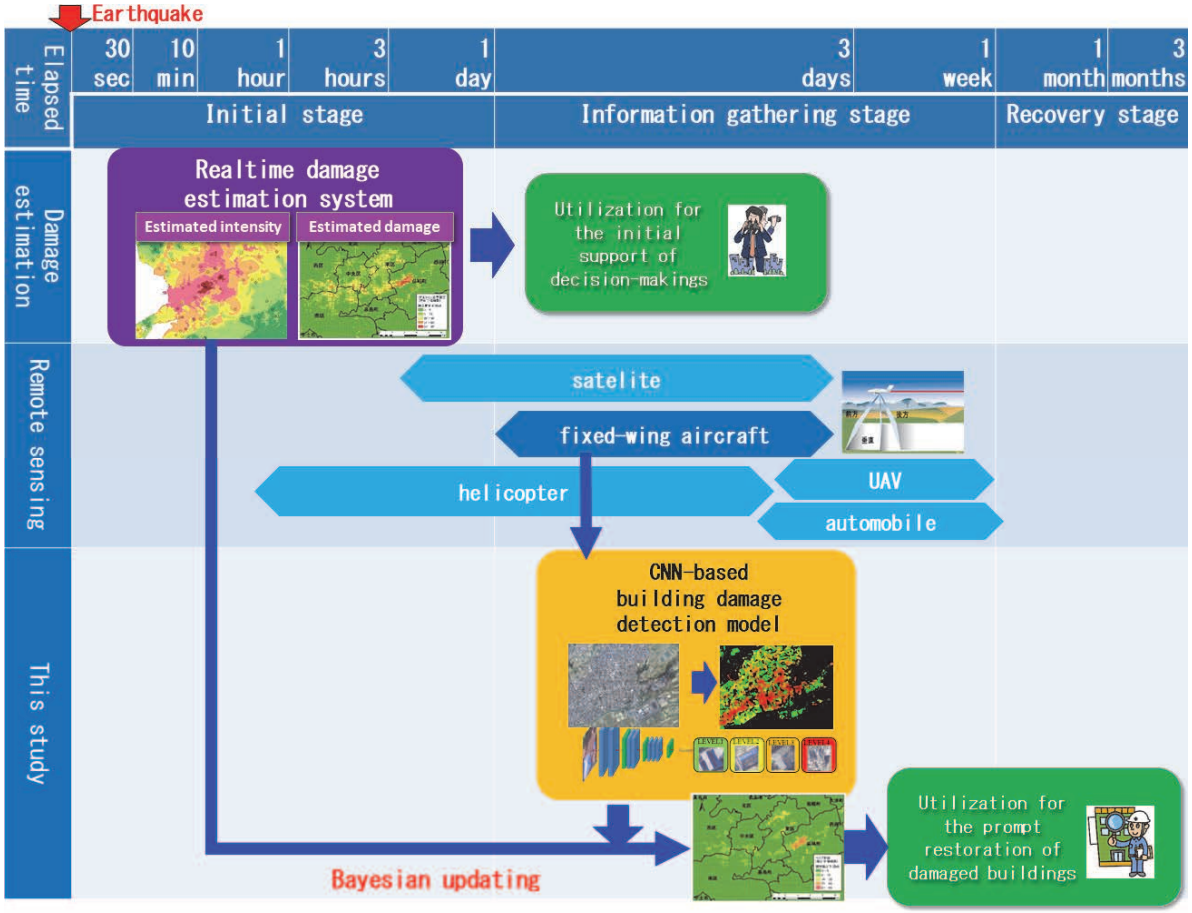

Fig. 1 – Overview of this study

2. Development of training data

The visual interpretation of aerial photography is an efficient means of detecting damaged buildings. Using the results of previous studies [11] [12], we defined a damage classification scale for buildings, and visually classified the damage to each building using photographs of the aftermath of the 2016 Kumamoto earthquake, which were taken from above by a fixed-wing airplane. These aerial photographs have a resolution of 20 cm per pixel, which is sufficient to classify the damage to each building into one of four levels. The damage classification scale is as follows: LEVEL 1: No damage, LEVEL 2: Minor damage, LEVEL 3: Moderate damage, LEVEL 4: Major damage (Table 1) [13]. Subsequently, we constructed GIS data labeled with each damage level using the building polygons released by the Geospatial Information Authority of Japan [14]. In accordance with the procedure noted above, we constructed more than 320,000 training data for building damage detection from aerial photographs of the 2016 Kumamoto earthquake (Table 2, Fig. 2).

Table 1 – Damage classification scale used in this study [10][13]

Classification	Features in photograph	Damage grade[11]
LEVEL1	No damage can be confirmed	D0
LEVEL2	Some roof tiles have collapsed	D1
LEVEL3	Most of the roof tiles have collapsed, or part of a wall has fallen	D2+D3
LEVEL4	Distortion of the entire building, destruction or collapse	D4+D5

Table 2 – Number of buildings used as training data in this study

Earthquake	LEVEL1	LEVEL2	LEVEL3	LEVEL4	total
2016 Kumamoto	240,316	68,699	9,057	2,090	320,162

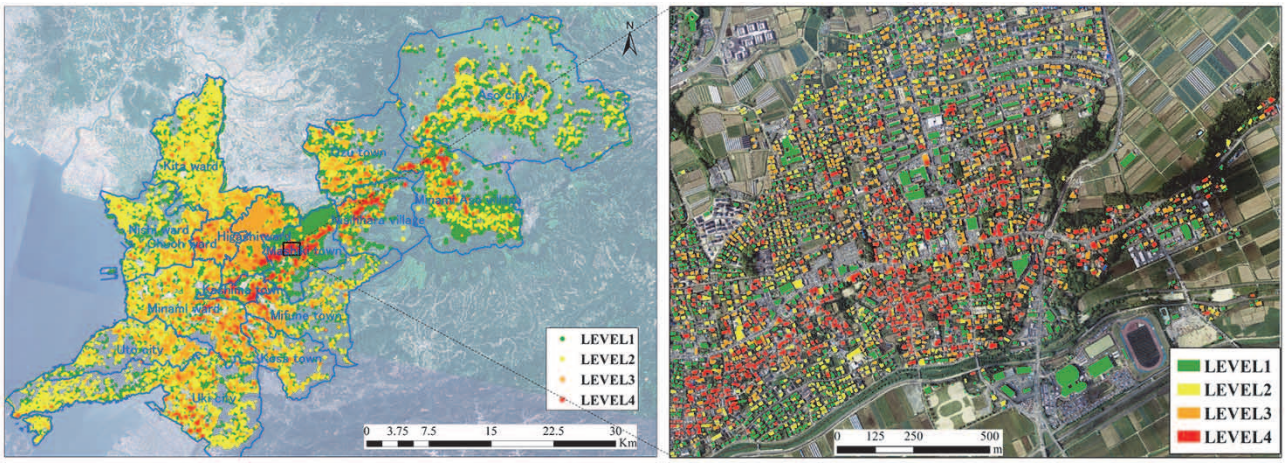

Fig. 2 – Coverage of the training data generated by aerial photographs taken soon after the main shock of the Kumamoto earthquake (left), and magnification of the damaged area at Mashiki-town (right) [10]. Background photo is taken by Geospatial Information Authority of Japan (GSI) (left) and Pasco Corp. (right).

The building damage classification scale in this study was validated through a comparison with a field investigation performed at Mashiki-town [15], in which the exterior appearance of buildings was classified using the building damage pattern chart developed by Okada and Takai [11]. Comparisons in the same area suggest that the distribution of collapsed buildings (D4 or D5) is similar to the concentrated area of LEVEL 4 damage (Fig. 3).

The confusion matrix of the field inspection and visual interpretation of the aerial photography is presented in Table 3. According to this matrix, the precision and recall of LEVEL 1 damage are greater than 71%, and those of LEVEL 4 damage are greater than 73%; the precision and recall of the other levels range from 30–44%. These results show that the proposed method seems to be especially good at detecting collapsed buildings. Therefore, we think that the visual judgment of aerial photography is sufficiently reliable for supporting the disaster response efforts of municipalities and companies. In the initial stages of the disaster response, accurate estimations of the distribution and concentration of collapsed buildings is important for estimating the resources needed for restoration.

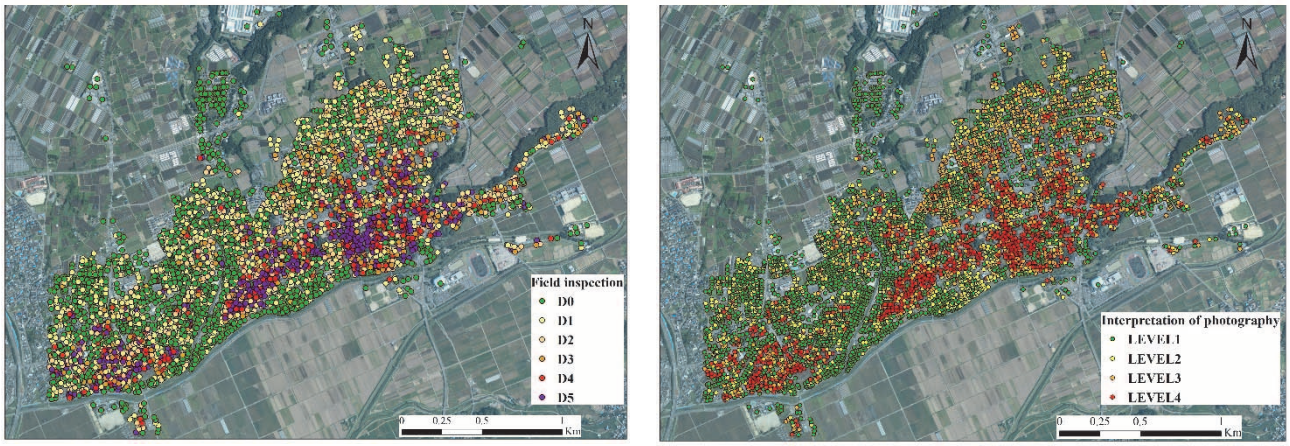

Fig.3 – Comparison of the building damage in Mashiki-town classified by field inspections [15] (left) and visual interpretation of photographs (right) [13]. Background photos taken by GSI.

Table 3 – Confusion matrix between the field inspection and the visual interpretation of aerial photography

		Visual interpretation of the aerial photography				total	Recall (%)	F-measure (%)
		LEVEL1	LEVEL2	LEVEL3	LEVEL4			
Field inspection	D0	1,878	237	69	21	2,205	85.2	77.7
	D1	470	409	414	39	1,332	30.7	36.1
	D2+D3	223	213	458	180	1,074	42.6	43.3
	D4+D5	59	72	102	676	909	74.4	74.1
total		2,630	931	1,043	916	5,520	-	-
Precision(%)		71.4	43.9	43.9	73.8	Overall accuracy(%)		62.0

3. CNN-based damage detection model

As discussed in [10], we developed a building damage detection model based on the visual geometry group (VGG) model [16]. In training the model, a number of 80×80-pixel image patches (corresponding to a real size on the ground of approximately 20×20-m), including most parts of the buildings, were automatically cropped from the aerial photography (Fig. 4). Subsequently, iterative CNN calculations were performed using these image patches. The construction of the damage detection model is completed by optimizing the parameters. In the discrimination stage, the entire area covered by the aerial photography is raster-scanned, and pixel-based damage detection is performed by applying the model to each 80×80-pixel image patch. Subsequently, all buildings in the photograph were automatically classified into one of four damage levels using the thresholds described in Table 4 in descending order based on the area ratio of pixel-based damage detected within each building polygon.

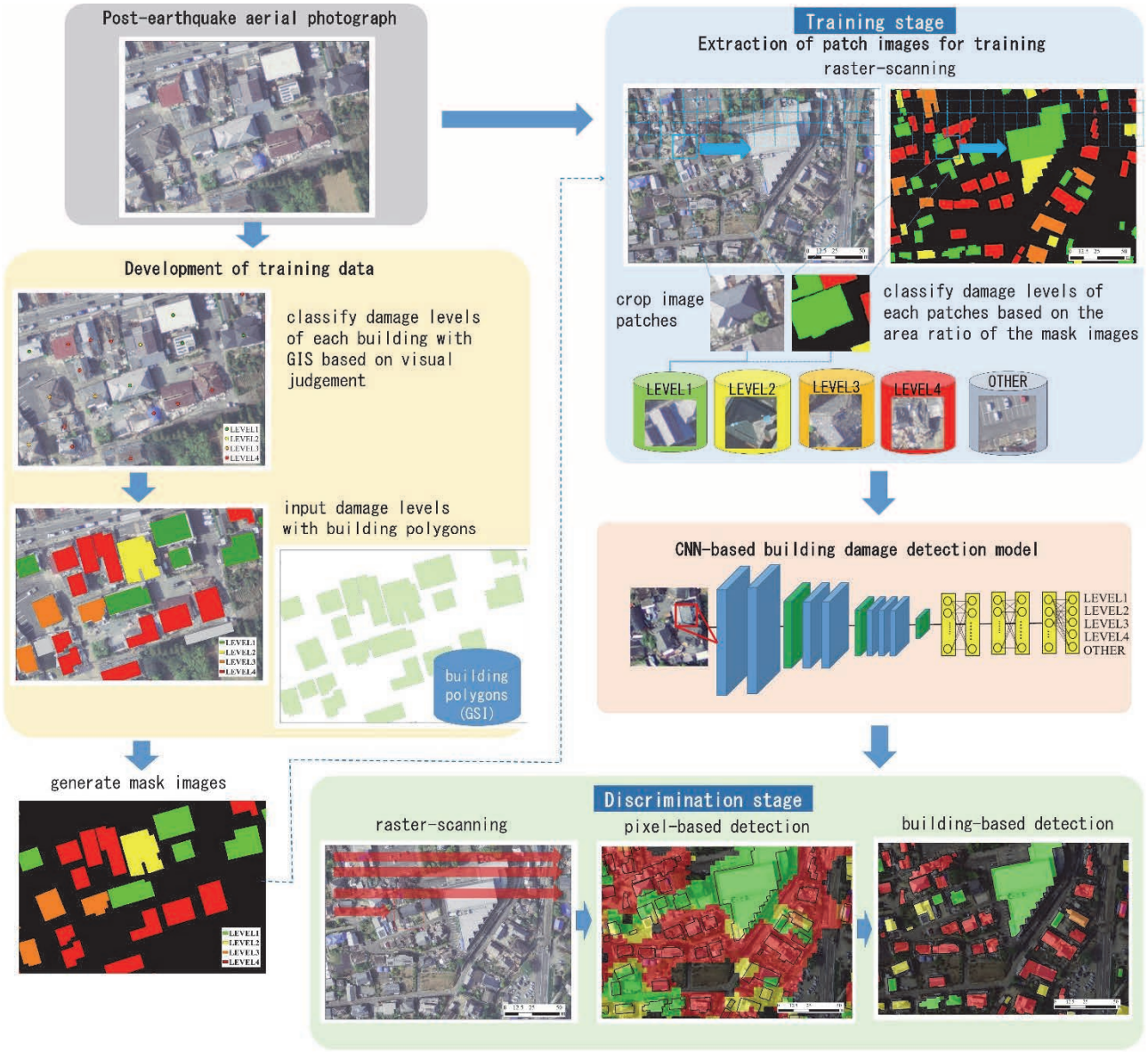

Fig. 4 – CNN-based building damage detection model [10]

Table 4 – Threshold of building-based damage detection

Priority	Classification	Threshold
4	LEVEL1	Other
3	LEVEL2	Including LEVEL2 30% or more
2	LEVEL3	Including LEVEL3 10% or more
1	LEVEL4	Including LEVEL4 10% or more

In our previous study [10], we developed the CNN-based damage detection model using 2,500 image patches as training data for each damage level. All image patches were cropped from photographs of the aftermath of the Kumamoto earthquake, as illustrated on the right of Fig. 2. Subsequently, we performed building-based

damage detection using 20 photographs taken at the same time (Fig. 5). The results of the CNN-based damage detection model are illustrated on the right of Fig. 5 [10], and the visual interpretation of the aerial photography is on the left. Comparatively, the area of collapsed buildings (LEVEL 4) in the right-hand figure seems to be slightly large. However, both figures clearly indicate concentrated lines of LEVEL 4 damage along the central part of Mashiki-town.

Furthermore, we evaluated the accuracy of our model by constructing a confusion matrix between the visual interpretation results and building-based damage detection results illustrated in Fig. 5. As a result, the recall of each damage level was found to range from approximately 57–85%, with especially high recall for LEVEL 4 damage. However, the precision was relatively low, especially at LEVEL 2 and LEVEL 4 (Table 5). In this case, we think the recall is more suitable for evaluation. Because the number of buildings classified into each level is unequal, the misclassification of LEVEL 1 impacts the precision of the other classes. Additionally, in the early stages of disaster response, estimating the number of collapsed buildings is essential for making decisions regarding the prioritization of manpower and resources. For these reasons, we believe that the CNN-based damage detection model is suitable for disaster response.

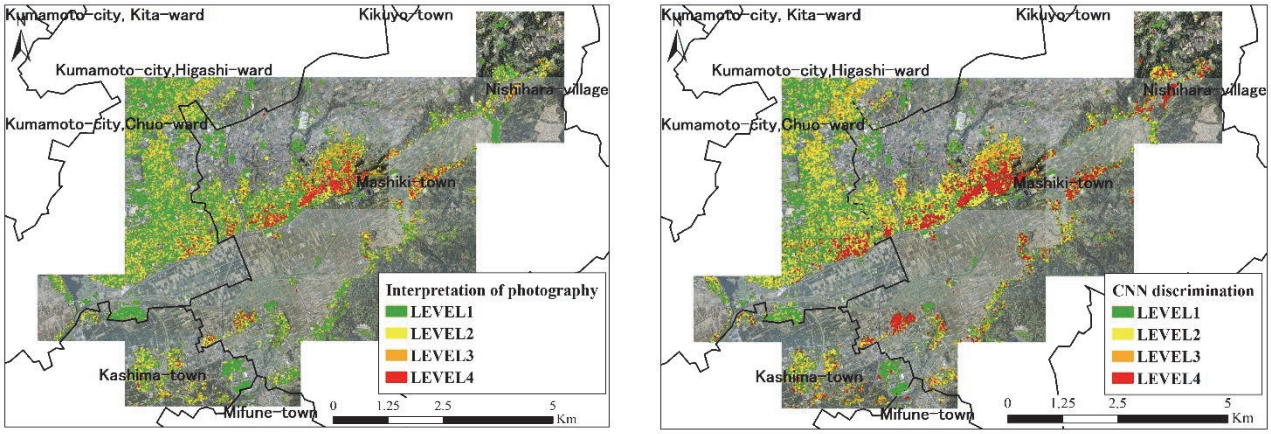

Fig.5 – Comparison of the building damage of Mashiki-town classified by visual interpretation of aerial photography (left) and building-based damage detection using CNN model (right) [10]. Background photos taken by Pasco Corporation.

Table 5 – Confusion matrix between the visual interpretation results of aerial photographs and building-based damage detection results using CNN model [10]

		discrimination result using CNN model				total	Recall (%)	F-measure (%)
		LEVEL1	LEVEL2	LEVEL3	LEVEL4			
visual interpretation	LEVEL1	14,295	3,094	451	840	18,680	76.5	83.1
	LEVEL2	1,247	3,477	654	484	5,862	59.3	53.6
	LEVEL3	139	443	1,446	502	2,530	57.2	56.2
	LEVEL4	62	90	63	1,257	1,472	85.4	55.2
total		15,743	7,104	2,614	3,083	28,544	-	-
Precision(%)		90.8	48.9	55.3	40.8	Overall accuracy(%)		71.7

4. Bayesian updating method

J-RISQ [1][2] is a real-time damage estimation system that uses more than 5,000 strong motion observation stations in Japan. The observed seismic intensities are interpolated on a 250×250-m mesh using a mathematical formula [17] and site amplification factors [18] [19]. The number of collapsed buildings in each cell of the mesh is then estimated based on a building database constructed from residential maps [20] and plural damage functions [21][22][23][24] (Fig. 6).

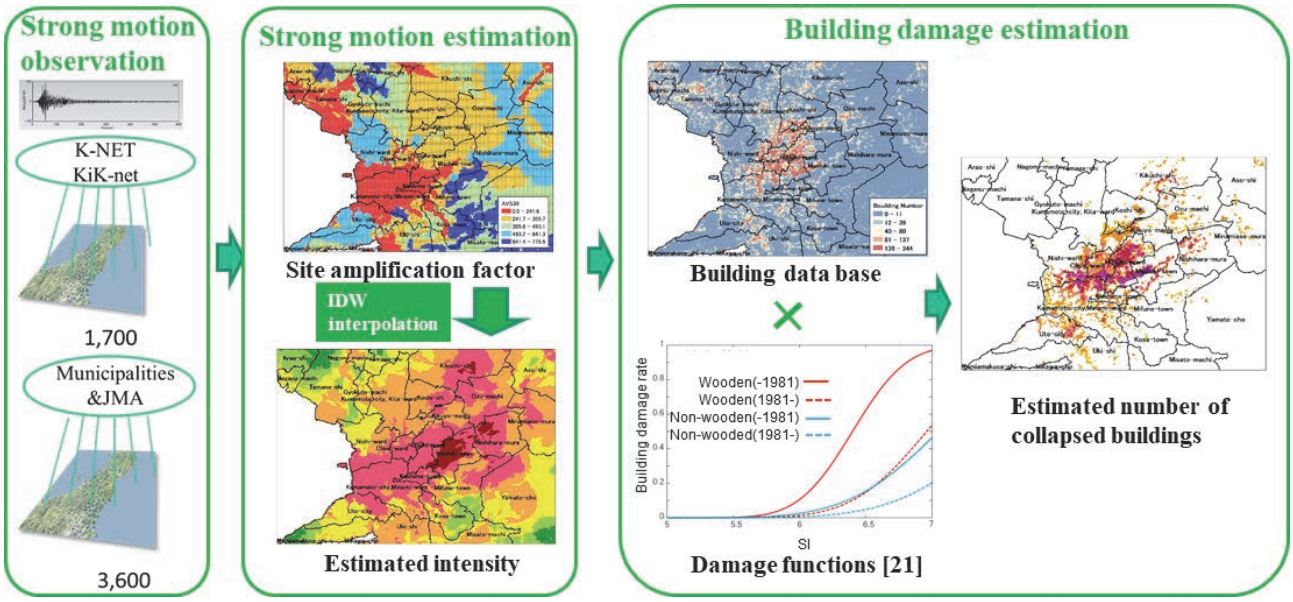

Fig. 6 – Overview of the real-time damage estimation system J-RISQ

The estimated seismic intensity is not always reflected in the regional site amplification, and an estimation model based on a fragility curve has a degree of uncertainty. Thus, the estimated results are sometimes different to the actual damage. Additionally, remote sensing images for local governments and companies are sometimes only partially available, and damage information gradually changes over time. Therefore, for prompt disaster response, fragmentary damage information must be aggregated and real-time damage estimation should be updated using remote sensing images. To this end, we combined the Bayesian updating method of J-RISQ [25] with the estimation results of the CNN-based damage detection model (Fig. 7).

In the Bayesian updating method, the damage probabilities of collapsed buildings $p_{h,i}(\theta)$ and structurally damaged buildings $p_{m,i}(\theta)$ calculated by J-RISQ for mesh cell i are used as prior probabilities. Each probability is defined as a cumulative standard normal distribution (ϕ), described with the parameters of estimated seismic intensity s_i , average μ_h , μ_m and standard deviation σ_h , σ_m , and an error parameter θ (see Eqs. (1) and (2)). Subsequently, each probability is updated to a posterior collapsed probability of $p_h(\theta|d_{h,i})$ (Eq. (3)) and a structurally damaged probability $p_m(\theta|d_{m,i})$ (Eq. (4)) through multiplication by the likelihood function $L(\theta)$. In this case, c_h and c_m are constant numbers used for normalization. Furthermore, the likelihood function $L(\theta)$ is composed of a polynomial distribution using the average ratios of the damage probability of collapsed buildings $\bar{p}_{h,i}$ and structurally damaged buildings $\bar{p}_{m,i}$, and each probability is weighted by the number of buildings n_i in each cell (Eqs. (5) and (6)). Furthermore, the numbers of collapsed buildings $d_{h,i}$ and structurally damaged buildings $d_{m,i}$ are generated by aggregating the CNN-based damage detection results in each cell from the post-earthquake aerial photography using the likelihood function $L(\theta)$ (Eq. (7)) , Eqs. (3) and (4).

$$p_{h,i} = \phi((s_i - \mu_h + \theta)/\sigma_h) \tag{1}$$

$$p_{m,i} = \phi((s_i - \mu_m + \theta)/\sigma_m) \tag{2}$$

$$p_h(\theta|d_{h,i}) = c_h \cdot L(\theta) \cdot p_{h,i}(\theta) \tag{3}$$

$$p_m(\theta|d_{m,i}) = c_m \cdot L(\theta) \cdot p_{m,i}(\theta) \tag{4}$$

$$\bar{p}_{h,i} = \sum_i n_i p_{h,i} \Big/ \sum_i n_i \tag{5}$$

$$\bar{p}_{m,i} = \sum_i n_i p_{m,i} \Big/ \sum_i n_i \tag{6}$$

$$L(\theta) \propto \prod_{i=1}^{N} \bar{p}_{h,i}{}^{d_{h,i}} \cdot \left(\bar{p}_{m,i} - \bar{p}_{h,i}\right)^{d_{m,i}-d_{h,i}} \cdot \left(1 - \bar{p}_{m,i}\right)^{n_i - d_{m,i}} \tag{7}$$

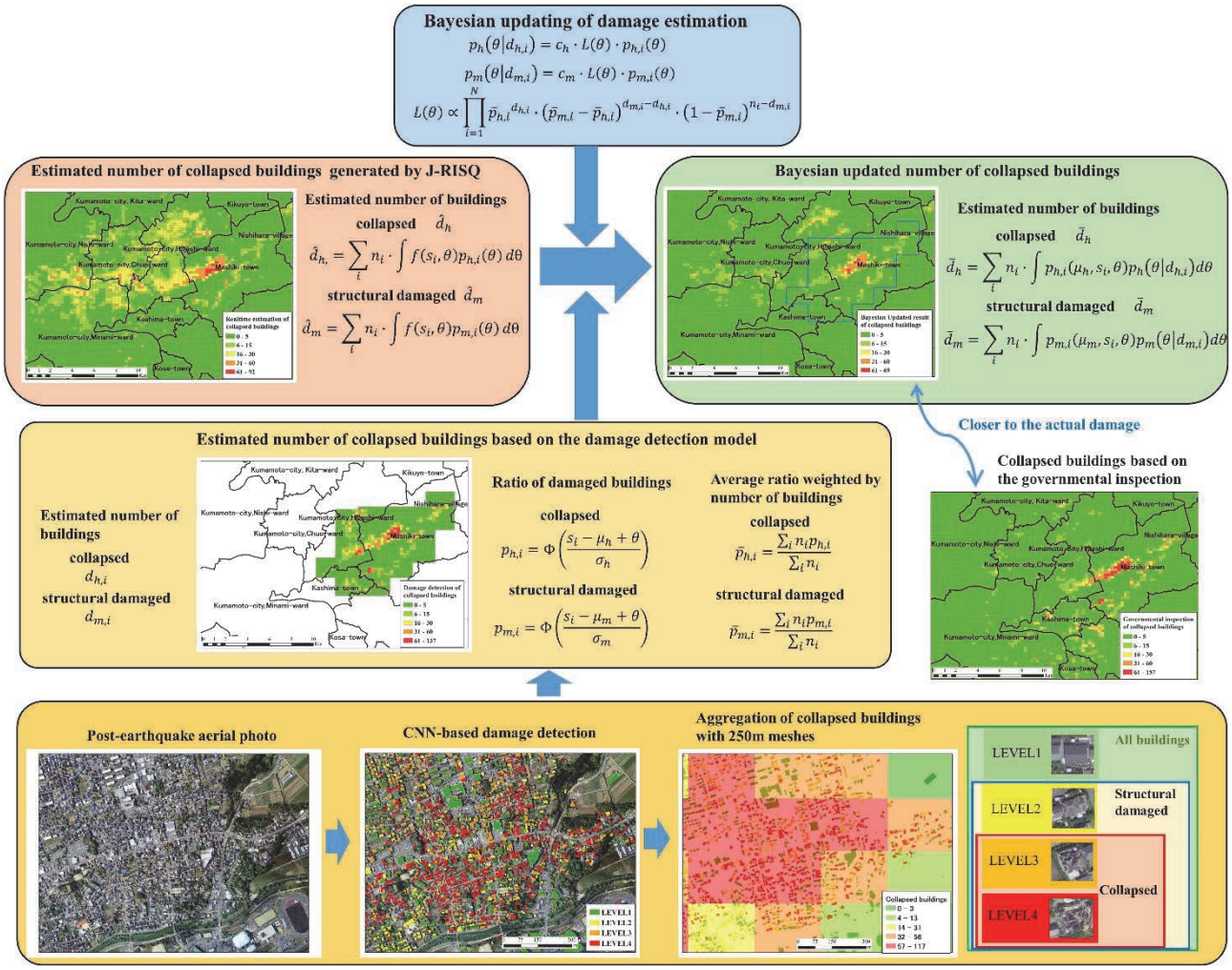

Fig. 7 – Bayesian updating method of the real-time damage estimation

In this method, the number of damaged buildings in each 250×250-m cell is aggregated. LEVEL 3 and above is taken to represent collapsed buildings, with LEVEL 2 and above representing structurally damaged buildings. Additionally, we used the Metropolis–Hastings algorithm, which is a Markov Chain Monte Carlo (MCMC) method. The MCMC parameters are presented in Table 6.

In the case of the main shock of the Kumamoto earthquake, the real-time results given by J-RISQ [22] were overestimated compared to a governmental field survey [26], especially in Nishi-ward, Chuo-ward, Higashi-ward, and Minami-ward of Kumamoto city (Fig. 8). However, using the proposed Bayesian updating method with aerial photos covering part of Higashi-ward, Kashima-town, and Mashiki-town, the degree of overestimation in Kumamoto city was reduced (Fig. 9, Table 7). Additionally, the number of totally collapsed buildings and structurally damaged buildings in Kumamoto city came closer to the governmental inspection result [26] (Fig. 10, Table 7).

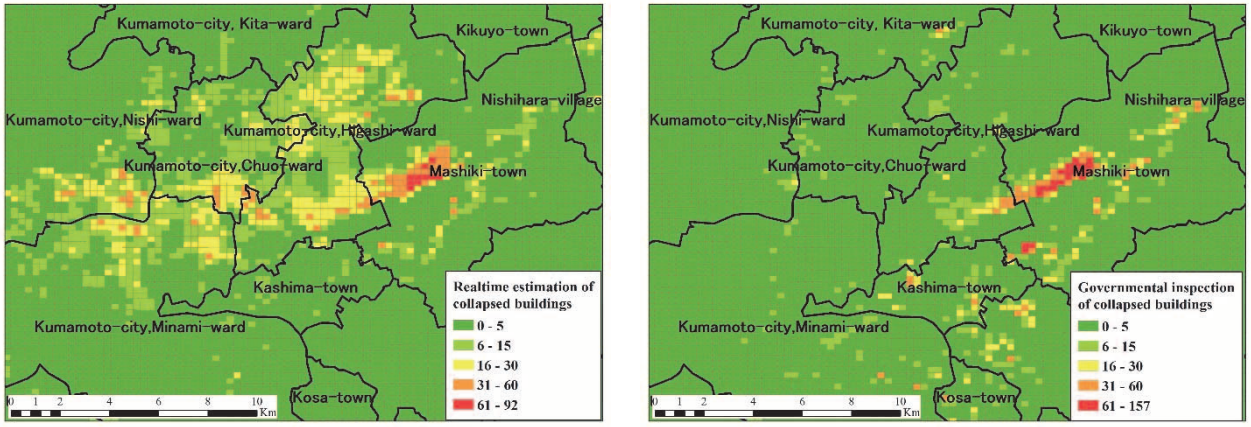

Fig. 8 – Collapsed buildings estimated by J-RISQ (left) and governmental inspection result of collapsed buildings (right) [27]

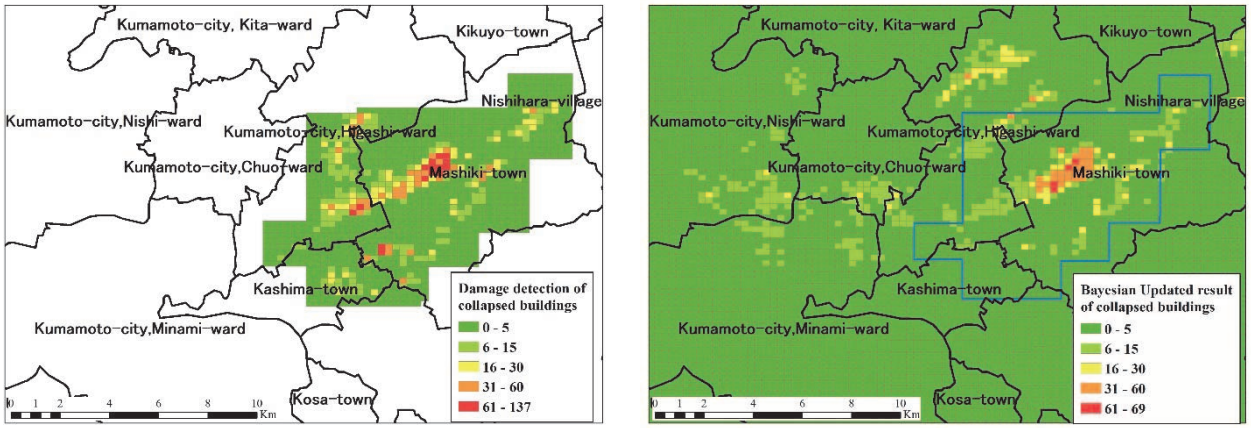

Fig. 9 – Collapsed buildings detected by CNN-based model (left) and Bayesian updated result of collapsed buildings (right) [27]

Table 6 – Parameters of MCMC

MCMC sample size	30,000
Burn in	20,000
Standard deviation of MCMC step width	0.01
Average (μ) of prior distribution $p(\theta)$	0
Standard deviation (σ) of prior distribution $p(\theta)$	0.1

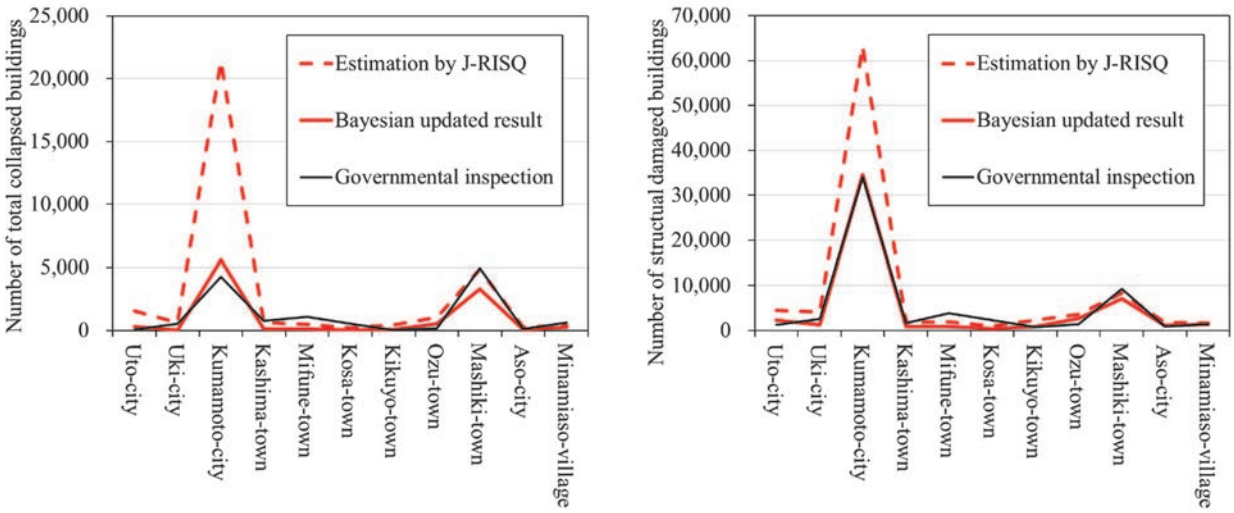

Fig. 10 – Number of collapsed buildings (left) and structurally damaged buildings (right) per municipality estimated by J-RISQ, Bayesian updating, and governmental inspection

Table 7 – Summation of totally collapsed buildings (left) and structurally damaged buildings (right) per municipality (EST: estimation by J-RISQ; BYS: Bayesian updated result; GOV: governmental inspection)

	Total collapsed buildings			**Structural damaged buildings**		
Municipality	EST[22]	BYS	GOV[26]	EST[22]	BYS	GOV[26]
Uto-city	1,535	299	96	4,562	2,358	1,277
Uki-city	607	48	534	4,096	1,311	2,599
Kumamoto-city	21,400	5,615	4,244	63,228	34,582	34,074
Kashima-town	606	122	753	1,754	918	1,696
Mifune-town	486	143	1,109	1,962	882	3,874
Kosa-town	201	22	512	1,020	396	2,283
Kikuyo-town	427	67	28	2,332	884	833
Ozu-town	1,025	541	148	3,625	2,767	1,462
Mashiki-town	4,856	3,287	4,973	8,403	7,117	9,223
Aso-city	274	66	101	1,792	1,221	903
Minamiaso-village	376	242	623	1,650	1,413	1,467
Total	31,793	10,452	13,121	94,424	53,849	59,691

5. Conclusion

We have developed a CNN-based damage detection model for prompt disaster response using post-earthquake aerial photography. With this model, the numbers of totally collapsed buildings and structurally

damaged buildings were clearly estimated using aerial photos taken soon after the main shock of the Kumamoto earthquake. We constructed a likelihood function using these damage detection results, and applied a Bayesian updating method to the real-time damage estimation result given by J-RISQ. Using this method, the updated results for damaged buildings were closer to the results of governmental inspections.

We believe that the proposed Bayesian updating method can be used to support disaster response efforts, because updated damage information is helpful to anyone engaged in disaster response, such as municipalities and insurance companies. This information is also useful for making prompt decisions, such as prioritizing the assignment of manpower or arranging relief supplies.

6. Acknowledgements

This study was supported by the Cross-ministerial Strategic Innovation Promotion Program, entitled "Enhancement of societal resiliency against natural disasters", under the initiative of the Cabinet Office, Government of Japan. We thank Dr. Akihiro Kusaka for cooperation of developing the Bayesian updating method of J-RISQ. We thank Stuart Jenkinson, PhD, from Edanz Group for editing a draft of this manuscript.

7. References

[1] Fujiwara H, Nakamura H, Senna S, Otani H, Tomii N, Ohtake K, Mori T, and Kataoka S (2019): Development of a real-time damage estimation system. *Journal of Disaster Research,* **14** (2), 315-332.

[2] Nakamura H, Fujiwara H, Kunugi T, Aoi S, Senna S, Takahashi I, Naito S, and Azuma H (2017): Development of real-time earthquake damage information system in Japan. *in Proceeding, 16th World Conference on Earthquake Engineering (16WCEE),* 9-13 January, 2017, Santiago, Chile.

[3] Matsuoka M and Nojima N (2010): Building damage Estimation by integration of seismic intensity information and satellite L-band SAR imagery. *Remote Sensing,* **2010**(2), 2111-2126.

[4] Menderes A, Erener A, and Sarp G (2015): Automatic detection of damaged buildings after earthquake hazard by using remote sensing and information technologies. *Procedia Earth and Planetary Science* **15**, 257–262.

[5] Vetrivel A, Gerke M, Kerle N, and Vosselman G (2016): Identification of structurally damaged areas in airborne oblique images using a Visual-Bag-of-Words approarch. *Remote Sensing* **8**(231).

[6] LeCun Y, Boser B, Denker J S, Henderson D, Howard R E, Hubbard W, and Jackel L D (1989): Backpropagation applied to handwritten zip code recognition. *Neural Computation* **1**, 541-551.

[7] Fujita A, Sakurada K, Imaizumi T, Ito R, Hikosada S, and Nakamura R (2017): Damage detection from aerial images via Convolutional Neural Networks. *15th IAPR International Conference on Machine Vision Applications*.

[8] Vetrivel A, Gerke M, Kerle N, Nex F, and Vosselman G (2017): Disaster damage detection through synergistic use of deep learning and 3D point cloud features derived from very high resolution oblique aerial images, and multiple-kernel learning. *ISPRS Journal of Photogrammetry and Remote Sensing*, http://dx.doi.org/10.1016/j.isprs.2017.03.001

[9] Ishii Y, Matsuoka M, Maki N, Horie J. and Tanaka S (2018): Recognition of damaged building using deep learning based on aerial and local photos taken after the 1995 Kobe Earthquake. *Journal of structural and construction engineering*. **83**(751), 1391-1400. (in Japanese)

[10] Naito S, Tomozawa H, Mori Y, Nagata T, Monma N, Nakamura H, Fujiwara H, and Shoji G (2020): Building damage detection method based on machine learning utilizing aerial photographs of the Kumamoto Earthquake. *Earthquake Spectra*, in print.

[11] Okada S and Takai N (2000): Classification of structural types and damage patterns of buildings for earthquake field investigation. *in Proceedings, 12th World Conference on Earthquake Engineering (12WCEE)*, Paper No.705, Auckland, New Zeeland.

[12] Ogawa N and Yamazaki F (2000): Photo-interpretation of building damage due to earthquakes using aerial photographs. *in Proceedings of the 12th World Conference on Earthquake Engineering (12WCEE)*, Paper No.1906, Auckland, New Zeeland.

[13] Naito S, Monma N, Nakamura H, Fujiwara H, Shimomura H, and Yamada T (2018): Investigation of building damages caused by the 2016 Kumamoto earthquake utilizing aerial photographic interpretation. *Journal of JSCE A1*, **74**(4), 464-480. (in Japanese)

[14] Geospatial Information Authority of Japan (2018): Basic geographic data of Japan, available at http://www.gsi.go.jp/kiban/index.html (last accessed 9 November 2018).

[15] Naito S, Hao K X, Senna S, Saeki T, Nakamura H, Fujiwara H, and Azuma T (2017): Investigation of damages in immediate vicinity of co-seismic faults during the 2016 Kumamoto earthquake. *Journal of Disaster Research*, **12**(5), 899-915.

[16] Simonyan K and Zisserman A (2014): Very deep convolutional networks for large-scale image recognition. *arXiv:1409-1556*.

[17] Fujimoto K and Midorikawa S (2005): Empirical method for estimating J.M.A. instrumental seismic intensity from ground motion parameters using strong motion records during recent major earthquakes. *Institute of Social Safety Science*, **7**, 241-246 (in Japanese with English abstract).

[18] Fujimoto K and Midorikawa S (2006): Relationship between average shear-wave velocity and site amplification inferred from strong motion records at nearby station pairs. *Journal of Japan Association for Earthquake Engineering*, **6**(1), 11-22 (in Japanese with English abstract).

[19] Fujiwara H, Morikawa N, and Okumura T (2013): Seismic hazard assessment for Japan: Reconsiderations after the 2011 Tohoku Earthquake, *Journal of Disaster Research*, **8**(5), 848-860.

[20] ZENRIN Corporation (2019): Zmap-Town II, *https://www.zenrin.co.jp/english/index.html* [assessed December 12, 2019].

[21] Central Disaster Management Council (2004): *http://www.bousai.go.jp/jishin/syuto/pdf/shiryou3.pdf* (in Japanese) [accessed December 24, 2019]

[22] Central Disaster Management Council (2012): Outline of damage estimation items and estimation methods of building damage and causalities by the Nankai Trough Big Earthquake, *http://www.bousai.go.jp/jishin/nankai/taisaku wg/pdf/20120829 gaiyou.pdf* (in Japanese) [accessed December 24, 2019]

[23] Murao O and Yamazaki F (2002): Building Fragility Curves for the 1995 Hyogoken-nanbu Earthquake Based on CPIJ & AIJ's Survey Results with Detailed Inventory, Journal of Structural and Construction Engineering, **555**, 185-196 (in Japanese with English abstract).

[24] Midorikawa S, Ito Y, and Miura H (2011): Vulnerability Functions of Buildings based on Damage Survey Data of Earthquakes after the 1995 Kobe Earthquake, *Journal of JAEE,* **11**(4), 34-47 (in Japanese with English abstract).

[25] Kusaka A, Nakamura H, Fujiwara H, and Okano H (2017): Bayesian updating of damaged building distribution in post-earthquake assessment. *Earthquake Journal of Japan Association for Earthquake Engineering* **17**(1), 16–29 (in Japanese).

[26] Monma N, Nakamura H, Fujiwara H, Naito S, Shimomura H, and Yamada T (2018): Construction of earthquake building damage information space database and examination of building damage curve, *The 15th Japan Earthquake Engineering Symposium*, PS1-01-33, 2924-2933 (in Japanese).

[27] Naito S, Nakamura H, Fujiwara H, Kusaka A, Tomozawa H, Mori Y, Monma N, and Shoji G (2019): Updating method of the realtime damage estimation utilizing the automatic building damage detection method constructed with the deep learning of aerial photographs and investigation of applicability for the disaster response, *Proceedings of the ninth symposium on disaster mitigation and resilience of infrastructures and lifeline systems*, Paper No.9, 43-56, Okinawa, Japan (in Japanese).

